[68Ga]Ga-FAPI-46 synthesis on a GAIA® module system: thorough study of the automated radiolabeling reaction conditions

Léa Rubira, Charlotte Donzé, Juliette Fouillet, Benjamin Algudo, Pierre Olivier Kotzki, Emmanuel Deshayes, Cyril Fersing

Applied Radiation and Isotopes 206 (2024) 111211

Contents lists available at ScienceDirect

Applied Radiation and Isotopes

journal homepage: www.elsevier.com/locate/apradiso

[^{68}Ga]Ga-FAPI-46 synthesis on a GAIA® module system: Thorough study of the automated radiolabeling reaction conditions

Léa Rubira [a], Charlotte Donzé [a], Juliette Fouillet [a], Benjamin Algudo [a], Pierre Olivier Kotzki [a,b], Emmanuel Deshayes [a,b], Cyril Fersing [a,c,*]

[a] Nuclear medicine department, Institut régional du Cancer de Montpellier (ICM), Univ. Montpellier, Montpellier, France
[b] Institut de Recherche en Cancérologie de Montpellier (IRCM), INSERM U1194, Univ. Montpellier, Institut régional du Cancer de Montpellier (ICM), Montpellier, France
[c] IBMM, Univ Montpellier, CNRS, ENSCM, Montpellier, France

ARTICLE INFO

Keywords:
FAPI-46
Fibroblast
Automated production
Radiochemistry
Molecular imaging
Gallium-68

ABSTRACT

The influence of several parameters involved in the ^{68}Ga radiolabeling of FAPI-46 was studied at the scale of the automated reaction. Among the buffers tested, HEPES 0.3 M pH 4 allowed both high radiochemical purity (RCP) and radiochemical yield (RCY), without prepurification of ^{68}Ga but after final purification of [^{68}Ga]Ga-FAPI-46 on a C_{18} cartridge. A longer reaction time did not show significant benefit on the RCP, while higher loads of FAPI-46 and gentisic acid as anti-radiolysis compound allowed better RCY.

1. Introduction

Over the past 20 years, gallium-68 PET imaging has raised increasing interest (Baum and Rösch, 2013), in direct relation to the special consideration given to the chemistry of this radioelement (Davey and Paterson, 2022). Obtained from a ^{68}Ge/^{68}Ga radioelement generator, some of which being available in GMP-grade quality (Lepareur, 2022), ^{68}Ga ($t_{1/2}$ = 67.7 min, β^+ = 89 %, electron capture = 11 %) allows in-house preparation activities (Hendrikse et al., 2022) particularly suitable for research and development purposes, facilitating the rapid translation of experimental PET imaging molecules to clinical use (Zhang et al., 2019). To ensure quality assurance (GMP) specifications and meet national regulatory requirements (Decristoforo et al., 2017), automated ^{68}Ga radiolabeling of experimental vector molecules has become a standard in clinic (Decristoforo, 2012). Such production method allows increased radiolabeling yields, reliable and robust preparation processes and also addresses radiation protection considerations (Kleynhans et al., 2020). To date, several models of synthesis modules are commercially available, based on the use of sterile tubing sets and GMP grade reagent kits. These reagent kits are made up to contain the pharmaceutical grade components and supplies most likely to allow efficient ^{68}Ga radiolabeling, nevertheless, these reagent kits do not offer flexibility to adapt the radiolabeling conditions to a given vector. As a consequence, the reaction conditions for ^{68}Ga radiolabeling of innovative PET radiopharmaceuticals are rarely studied in detail apart from parameters independent of the kit reagents (e.g. amount of vector, temperature and heating time).

In recent years, in conjunction with the widespread use of ^{68}Ga, the preclinical and clinical use of quinoline-based small molecules targeting tumor microenvironment has gained tremendous momentum for both molecular imaging (Huang et al., 2022) and targeted radionuclide therapy (Privé et al., 2023). These molecules are directed against the fibroblast activation protein (FAP), a membrane-bound prolyl-oligopeptidase of the dipeptidyl peptidase (DPP) family, specifically overexpressed by cancer-associated fibroblasts (CAFs) in over 90 % of human epithelial malignancies (Scanlan et al., 1994). Representing the major subpopulation of cells in the tumor stroma, CAFs could play an important role in resistance to treatment, immunosuppression, angiogenesis and tumor invasion by remodeling the extracellular matrix (Lindner et al., 2019). A metabolic cooperation between CAFs and cancer cells is also possible, sustaining tumor dynamics (Liang et al., 2022). Throughout the development of FAP inhibitors (FAPI), sequential modulations of their chemical structure have led to optimized compounds bearing a DOTA chelator for complexation of various radiometals (Fig. 1) (Jansen et al., 2013, 2014; Loktev et al., 2019). In particular, FAPI-46 seems to be the most attractive derivative to date, with regard to its excellent *in vivo* characteristics. This is supported by several reports describing, for [^{68}Ga]Ga-FAPI-46, clinical properties at

* Corresponding author. IBMM, Univ Montpellier, CNRS, ENSCM, Montpellier, France.
E-mail address: cyril.fersing@icm.unicancer.fr (C. Fersing).

https://doi.org/10.1016/j.apradiso.2024.111211
Received 20 October 2023; Received in revised form 19 January 2024; Accepted 25 January 2024
Available online 1 February 2024

least comparable to [^{18}F]FDG in the detection of a variety of cancers (Promteangtrong et al., 2022; Siripongsatian et al., 2022; Wegen et al., 2022, 2023). Automated radiolabeling of FAPI-46 with either ^{68}Ga for PET imaging (Alfteimi et al., 2022; Da Pieve et al., 2022; Spreckelmeyer et al., 2020a; Plhak et al., 2023) or ^{177}Lu for therapy (Eryilmaz and Kilbas, 2021; Cankaya et al., 2023) has been previously reported, however, the protocols described only apply to specific models of synthesis modules. Furthermore, modulation of the different parameters involved during radiolabeling has not been studied at the scale of the automated reaction, as it has been done for other ^{68}Ga imaging agents (Reverchon et al., 2020).

In this context, the influence of the reaction buffer, reaction time, anti-radiolysis compound, amount of vector and method of purification of the final product was studied in depth during the automated ^{68}Ga radiolabeling of FAPI-46 on a GAIA® synthesis module. Thereby, the reaction conditions allowing to reach the best radiochemical yields (RCY) and highest radiochemical purity (RCP) without pre-purification of the generator eluate have been identified.

2. Methods

2.1. Solvents, reagents and equipment

2.1.1. General considerations

All the chemicals used for the radiolabeling reactions were of the highest available purity grade and were purchased from Merck (Darmstadt, Germany). Water for injection (Eau pour prép. injectables 10 mL PROAMP®, Aguettan, France, and 100 mL Ecoflac, B. Braun, France) and sodium chloride 0.9 % (Chlorure de sodium PROAMP® 0,9 % 10 mL, Aguettan, France) were of pharmaceutical grade and ethanol (Éthanol AP-HP 96 % (v/v), AGEPS, France) was of Ph. Eur. grade. Radiolabeling optimization assays were conducted on a GAIA® V2 synthesis module (Elysia-Raytest, Germany) driven by the appropriate software (GAIA control, Elysia-Raytest, Germany) and using disposable cassettes for synthesis (Fluidic kit RT-01-H ABX, Advanced Biochemical Compounds, Germany). Between each automated radiolabeling assay, the cassette installed on the synthesis module was rinsed with water for injection (WFI) according to a dedicated automated sequence. The manifolds were then conserved for the next assay and the tubing was changed. Radiolabeling assays were performed with non-GMP grade FAPI-46 (MedChem Express, NJ, USA). A stock solution of 1 mg/mL FAPI-46 in WFI was initially prepared and aliquoted into Eppendorf tubes (Protein LoBind Tubes 1.5 mL) to get 30 µg/30 µL fractions, kept at −20 °C for a maximum storage time of 3 months. Gallium-68 was obtained in 0.1 N HCl solution under its [^{68}Ga]$GaCl_3$ form from a 1.85 GBq ^{68}Ge/^{68}Ga generator of pharmaceutical grade (GALLI AD®, Ire Elit, Belgium) and was not further purified. A minimal period of 4 h and not exceeding 24 h was allowed between 2 consecutive elutions. The [^{68}Ga]Ga-FAPI-46 production was conducted in a grade A shielded cell with a laminar air flow (MEDI 9000 Research 4R, LemerPax, La Chapelle-sur-Erdre, France), with both the automated synthesis module and the ^{68}Ge/^{68}Ga generator placed in the hot cell. The radioactivity in the product vial as well as the residual activity of the reaction vial, waste vial, purification cartridge and terminal filter were measured in a calibrated ionization chamber (CRC®-25R, Capintec, USA) and corrected to the end time of radiolabeling in order to calculate the RCY.

2.1.2. Buffer solutions preparation

The buffers tested were chosen with respect to their pKa value(s). The concentration used for each buffer was based on ^{68}Ga radiolabeling conditions described in the literature. Each buffer solution studied was prepared extemporaneously before radiolabeling assays. The correct amount of buffer was weighed on a calibrated precision balance (320XB, Precisa Gravimetrics, Switzerland) with a single-use plastic spatula into a sterile single-use type 1 glass bottle and solubilized in WFI. For each buffer solution, the pH was adjusted with 37 % HCl so that a defined 1.5 mL volume of this solution added to 1.1 mL of 0.1 N HCl (representing the volume of eluate provided by the GALLI AD® generator) could reach a pH close to 3.4, which is ideal for ^{68}Ga radiolabeling (Bauwens et al., 2010). Table 1 summarizes the main information on the buffer solutions tested for the preparation of [^{68}Ga]Ga-FAPI-46.

Table 1
Properties of the buffer solutions used in the [^{68}Ga]Ga-FAPI-46 radiolabeling assays.

Buffer	pKa value (s)	Molarity (M)	pH	Buffer volume set for reaction	Ref.
Sodium acetate	4.8	0.4	4	1.5	Alfteimi et al. (2022)
HEPES	3.0 7.6	0.3	4		Baur et al. (2014)
Sodium ascorbate	4.1 11.8	0.4	4.5		Spreckelmeyer et al. (2020)
Ammonium acetate	4.8 9.3	0.1	4.5		Meisenheimer et al. (2020), Daniel et al. (2023)
Sodium formate	3.8	1.5	3.5		de Blois et al. (2018)
Sodium succinate	4.2 5.6	0.5	4		Bauwens et al. (2010)

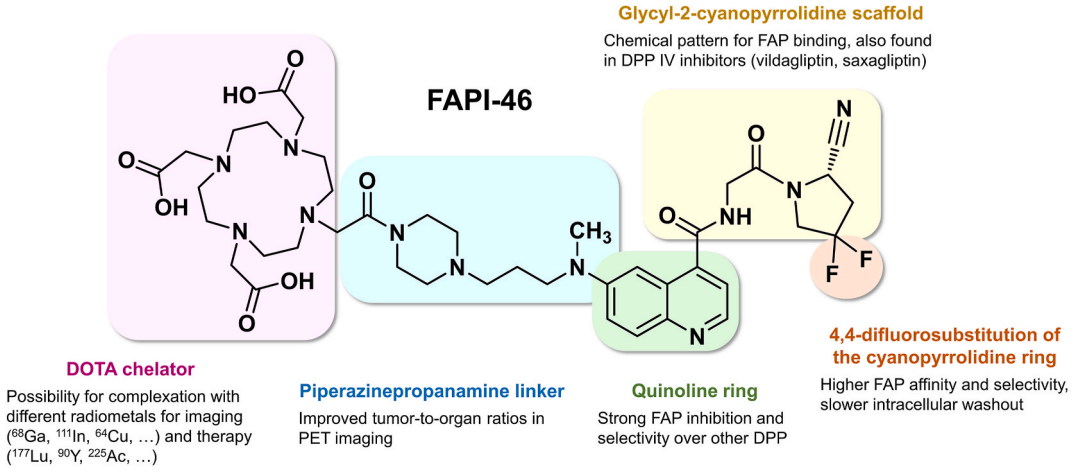

Fig. 1. Chemical structure and main structure activity relationships of FAPI-46.

2.2. Preparation for radiolabeling of FAPI-46 with gallium-68

First, the synthesis module was equipped with a disposable cassette according to the configuration described in Fig. 2. The GAIA® module is equipped with 15 manifolds, a heating block that receives the reaction vial, and a peristaltic pump to transfer liquids during the synthesis. If needed during the assay, purification cartridges were properly preconditioned, the corresponding eluents were prepared in syringes, and both were connected to the cassette. Finally, the correct amount of FAPI-46 (10–30 µL of 1 mg/mL aliquots in WFI) was added to 1.5 mL of the desired buffer solution and connected to the cassette. Each reaction conditions modification was studied by performing the related automated assay in triplicate, for a total of 45 runs. Values of RCP and RCY obtained for each triplicate were expressed as mean ± standard deviation.

- To study the influence of the reaction buffer, FAPI-46 was dissolved in a fixed 1.5 mL volume of different buffer solutions with strictly controlled pH (see Table 1) before starting the automated synthesis.
- To study the effects of a longer radiolabeling reaction time, the duration of the heating step was doubled (16 min instead of 8 min).
- To study the influence of an anti-radiolysis compound on the RCP over time, the buffer solution was added with 0.1 mL of freshly prepared ascorbic acid 10 mg/mL, gentisic acid 16 mg/mL or methionine 10 mg/mL solution. To ensure that the final preparation contained the same concentration of anti-radiolysis compound, the 8.6 mL of 0.9 % NaCl for terminal SPE cartridge elution were also supplemented with 570 µL of the corresponding anti-radiolysis compound solution. The stability of the final product [^{68}Ga]Ga-FAPI-46 at room temperature was then monitored, measuring RCP by radio-high-performance liquid chromatography (radio-HPLC) at 0.5, 1, 2, 3 and 4 h after the radiosynthesis.
- To study the influence of the amount of vector, radiolabeling assays were performed by adding 30, 20 or 10 µg of FAPI-46 in the buffer solution before starting the automated synthesis.
- To study the influence of the post-[^{68}Ga]Ga-FAPI-46 radiolabeling purification step, the cassette installed on the synthesis module was equipped with a solid phase extraction (SPE) cartridge (Sep-Pak® C_{18} or Oasis® HLB, Waters, USA), sequential SPE and quaternary methyl ammonium (QMA) cartridges (Waters Accell™ Plus QMA, Waters, USA) or no purification cartridge. SPE cartridges were preconditioned manually by washing successively with 5 mL of 96 % (v/v) ethanol and 5 mL of WFI; QMA cartridges were preconditioned manually by washing successively with 5 mL of potassium hydrogencarbonate 0.4 M and 5 mL of WFI.

2.3. Automated radiolabeling process of FAPI-46 with [^{68}Ga]GaCl$_3$

After initialization of the synthesis sequence, the module performs a kit integrity test to prevent any leakage during preparation. Then, the SPE cartridge is conditioned with WFI before the tubing lines are purged with filtered air. FAPI-46 contained in 1.5 mL of buffer solution is transferred to the reaction vial and the ^{68}Ge/^{68}Ga generator is eluted with 1.1 mL of 0.1 N HCl, the unprocessed eluate being transferred to the reaction vial pre-heated at 60 °C. The radiolabeling reaction proceeds for 8 min at a temperature of 97 °C. The reaction medium is then transferred to the SPE cartridge, with subsequent rinsing of the reaction vial and tubing with 10 mL WFI. Free $^{68}Ga^{3+}$, not retained by the SPE cartridge, is removed to the waste vial while [^{68}Ga]Ga-FAPI-46 is trapped on the cartridge. The active substance is then eluted from the cartridge to the product vial by alternating fractions of 60 % ethanol (1.5 mL total) and 0.9 % NaCl (8.6 mL total). The majority of ^{68}Ga colloids potentially formed during radiolabeling is retained on the cartridge. Sterilizing filtration is ensured by a 0.22 µ end filter (Millex®-GV 0.22 µ 1.3 cm, Merk, NJ, USA); integrity of the filter is checked by the module at the end of the preparation by a bubble point integrity test. The overall process of [^{68}Ga]Ga-FAPI-46 radiosynthesis with SPE purification step is summarized in Fig. 3 and the detailed automated sequence is provided in Supplementary materials.

2.4. Quality controls

2.4.1. TLC radiochemical purity assessment

Radio-thin layer chromatography (TLC) analyses were performed using 2 iTLC-SG strips (2 cm × 10 cm). A small drop of [^{68}Ga]Ga-FAPI-46 was placed on each strip 2 cm above the base line. The first strip was placed in a development chamber containing aqueous 1 M ammonium acetate in methanol (1:1) as mobile phase (conditions A); the second strip was placed in a chamber containing aqueous 0.1 M sodium citrate pH 5 as mobile phase (conditions B). The mobile phase was allowed to migrate approximately 1 cm below the top end of the strip. It was then removed from the chamber and placed into a TLC scanner (miniGITA® Star, Elysia-Raytest, Germany) to determine the % areas of radioactivity at the origin and at the solvent front, using the appropriate acquisition

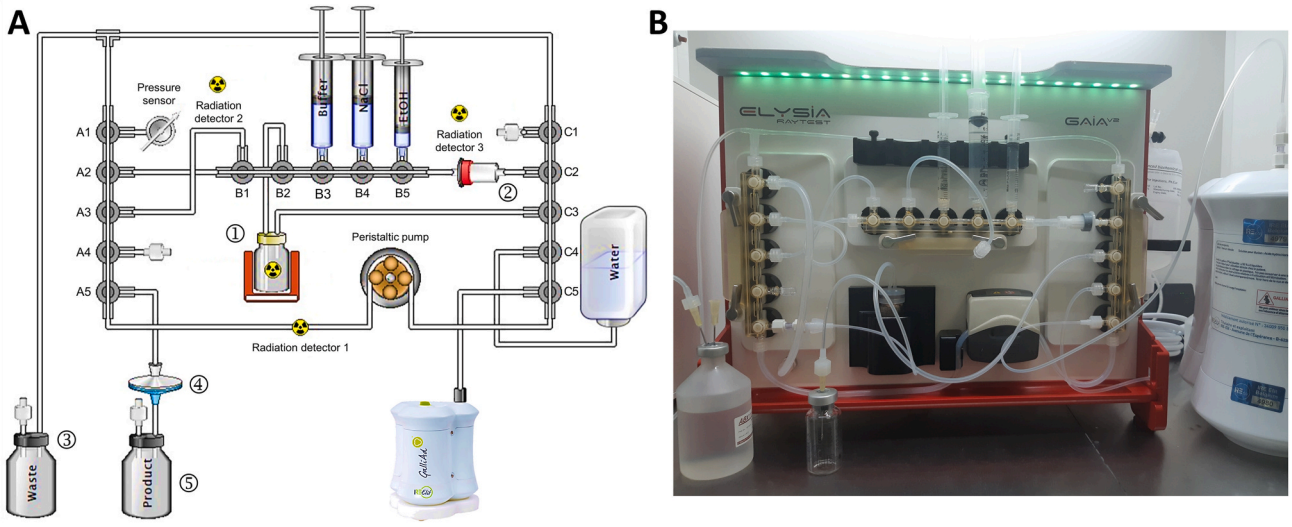

Fig. 2. A. Synthesis scheme for the automated production of [^{68}Ga]Ga-FAPI-46 using a GAIA® module; the main elements of the cassette are pointed out, namely ① the reaction vial, ② the purification cartridge, ③ the waste vial, ④ the terminal filter and ⑤ the product vial. **B**. Cassette mounted in the module, within the shielded cell.

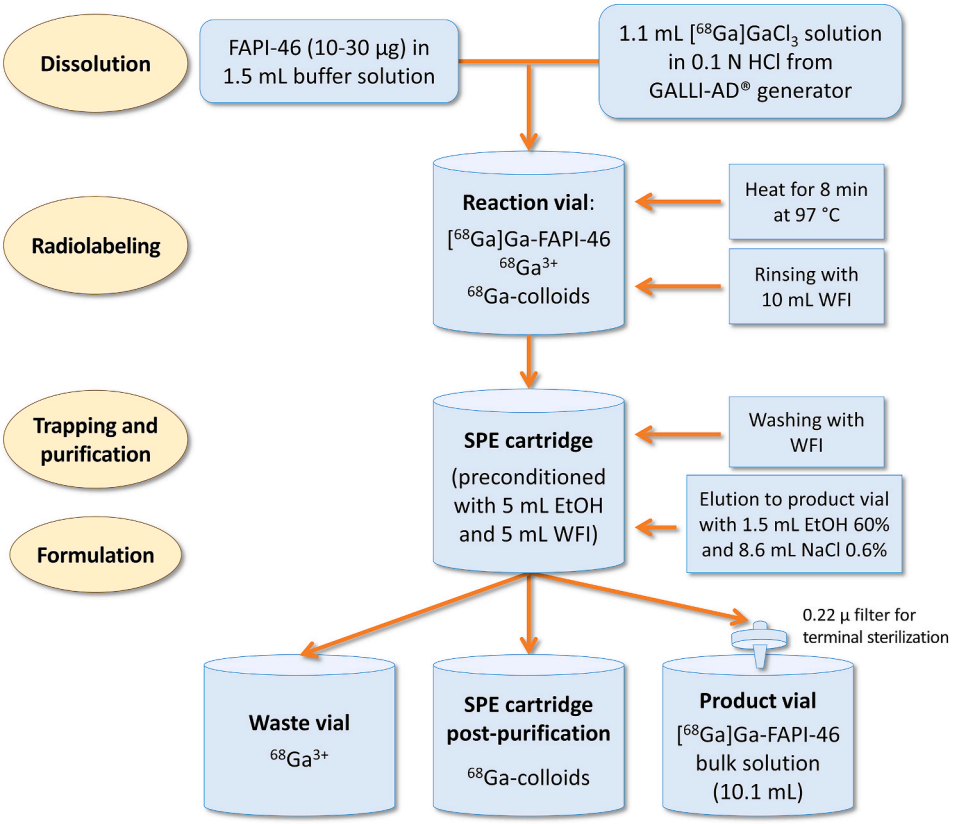

Fig. 3. Flow-chart of the [^{68}Ga]Ga-FAPI-46 radiosynthesis process.

software (TLC Control v.2.30, Raytest, Germany) and analysis software (GINA Star TLC™ v.6.0, Elysia-Raytest, Germany). In conditions A, R_f (^{68}Ga colloids) = 0.0–0.2 and R_f ([^{68}Ga]Ga-FAPI-46 + $^{68}Ga^{3+}$) = 0.8–1.0. In conditions B, R_f ($^{68}Ga^{3+}$) = 0.8–1.0 and R_f ([^{68}Ga]Ga-FAPI-46 + ^{68}Ga colloids) = 0.0–0.3.

2.4.2. HPLC radiochemical purity assessment

Radio-HPLC analyses were carried out on a Nexera X3 apparatus (Shimadzu, Japan) using HPLC-grade solvents. The radio-HPLC station consisted of a solvent degasser (DGU-405), a solvent pump (LC40D), an autosampler (SIL-40) set at 20 µL injection volume, a column oven (CTO-40S) set at 30 °C, a UV detector (SPD-40 190–700 nm) set at 254 and 280 nm and a radioactivity detector (GABI Nova with mid-energy probe and 2 × 5 µL flow cell) connected in series. The stationary phase was a C_{18} ACE® Equivalence™ column, 3.0 × 150 mm, 110 Å pore size and 3 µm particles size. The flow rate was 0.6 mL/min and the mobile phase gradient was programmed from 0.1 % TFA in water (A) to 0.1 % TFA in acetonitrile (B) as follow: 0–1 min 95/5 A/B; 1–8 min linear gradient from 95/5 A/B to 60/40 A/B; 8–9 min 60/40 A/B; 9–10 min linear gradient from 60/40 A/B to 95/5 A/B; 10–12 min 95/5 A/B. Radio-HPLC analyses were performed using the appropriate acquisition and analysis software (Gina Star 10, Elysia-Raytest, Germany).

2.4.3. pH evaluation

During buffer solutions preparation, pH was controlled using both 2-zones Rota pH 1–11 indicator paper (VWR, PA, USA) and MQuant® pH 2.5–4.5 indicator strips (Merk, NJ, USA). The pH of the final product [^{68}Ga]Ga-FAPI-46 was checked using only 2-zones Rota paper.

2.4.4. Determination of HEPES

The European Pharmacopoeia recently revised its specifications and requires a limit of 500 µg per injected dose for HEPES content in radiopharmaceuticals for parenteral administration (European Directorate for the Quality of Medicines & Healthcare (Edqm), 2021, 2022). Thus, the HEPES content was determined according to the standard TLC method listed in European Pharmacopoeia monographs. The following original TLC procedure, that was found more convenient and reproducible, was also used after optimization and validation (see Supplementary materials). Assuming that the maximum injectable volume can't exceed the final volume expected for the preparation (10.1 mL), a 49.5 µg/mL HEPES reference solution was prepared in a solvent mixture identical to the final preparation composition, i.e. NaCl 0.9 %/ethanol/WFI (8.6:0.9:0.6). Two separate spots (40 µL) of the reference solution and test solution (final [^{68}Ga]Ga-FAPI-46) were deposited with capillary tubes on a TLC silica gel F254 plate coated on aluminum foil (4 cm × 6 cm) and dried during 10 min in a 37 °C oven. The TLC was then developed in a chamber containing an acetone/water solution (4:1) as the mobile phase. The development was stopped when the front of the mobile phase was at 0.5 cm below the top end of the plate. Finally, HEPES was visualized after treatment of the developed TLC plate by exposure to iodine vapor. A 200 cm^3 hermetically sealed iodine chamber containing 2 g of solid iodine and 8 g of silica was used; complete burying of the TLC plate under the iodine/silica mixture for 5 min at 37 °C allowed optimal revelation. Any spot had to be less intense than the reference solution spot, consequently containing an HEPES amount lower than 49.5 µg/mL.

To confirm the HEPES content results obtained by TLC during method validation, an HPLC method for HEPES concentration determination was also implemented (see Supplementary materials) according to previously described procedures (Antunes et al., 2020; Migliari et al., 2022). Briefly, this method was set up on the same HPLC station used for radiochemical purity assessment. The mobile phase was 20 mM ammonium formate pH 9.5 at a 0.3 mL/min isocratic flow rate, for a total analysis time of 5 min. The injection volume was 20 µL and the UV detection was set at 220 nm.

2.5. Statistical analysis

Two-sided Wilcoxon rank sum test was used to compare triplicate RCP or RCY values obtained under two different reaction conditions. The p-value was used to estimate statistical significance.

3. Results and discussion

The fully-automated production of [^{68}Ga]Ga-FAPI-46 was completed in 24 min from the start of the synthesis to the delivery of the radiolabeled compound in the product vial. Since the transposition of a manual radiolabeling protocol on an automated module can require redesign and re-development of the process (Pisaneschi and Viola, 2022; Nelson et al., 2022), the study of several radiolabeling reaction parameters was directly conducted on automated syntheses. Therefore, the corresponding RCP and RCY values measured by both TLC and HPLC were compared. Of note, mean residual activity on the terminal filter over the 45 assays was 2.6 ± 1.4 MBq. Thus, it was considered negligible and was not taken into account in RCY calculations.

Firstly, 6 buffer solutions were evaluated through a protocol using 30 µg of FAPI-46 and final purification by C_{18} SPE cartridge. Fig. 4 summarizes the results obtained under these conditions; details on the distribution of the activity measured post-synthesis in the different components of the cassette are provided in *Supplementary data*. Sodium acetate 0.4 M pH 4 allowed only moderately good RCP, around 80 %, associated with modest RCY between 25 and 37 %. As observed in the literature, higher concentrations of this buffer is often associated with better results (Velikyan et al., 2017, 2020; Garcia-Arguello et al., 2019; Wagner et al., 2020). Ammonium acetate 0.1 M pH 4.5 slightly increased RCP (around 90 %) but caused a significant drop in RCY (around 16 %) due to a loss of activity in the reaction vial, in the waste vial and on the C_{18} cartridge. Sodium formate 1.5 M pH 3.5 slightly increased RCY (29–42 %) but still resulted in an important loss of $^{68}Ga^{3+}$ (approximately 50 %) in the waste vial, despite proper control of pH in the reaction medium. Similar results were observed with sodium ascorbate 0.4 M pH 4.5 (mean RCP around 96 % but mean RCY around 40 %). The use of sodium succinate 0.5 M pH 4 led to a considerable improvement of RCY (around 72 %) but was associated with poorly reproducible results, particularly for RCP controls by TLC. The best radiolabeling conditions were identified with HEPES 0.3 M pH 4 that allowed high RCP and RCY (around 95 % and 74 %, respectively) with little variation between the triplicate experiments. These excellent results are most probably related to the weak ability of HEPES to complex with metal ions (Ferreira et al., 2015), thus implying a wide use of this buffer in ^{68}Ga radiolabeling, but generally at a 5-fold higher concentration (Sammartano et al., 2020; Greiser et al., 2022; Hörmann et al., 2022; Migliari et al., 2023). Consequently, in our case, HEPES buffer was used for all subsequent assays. Through final SPE purification, a significant part of HEPES can be removed, with only traces remaining in the final product. Hence, although the initial amount of HEPES in the reaction medium was about 107 mg in 2.6 mL, a TLC control of the HEPES content in the previous triplicate experiments consistently showed a concentration in the final product around 10 µg/mL (quantified by HPLC dosing method), below the Ph. Eur. threshold of 49.5 µg/mL (500 µg in 10.1 mL).

Increasing the reaction time from 8 to 16 min showed a slight improvement in RCY (75.3 %–82.6 % in TLC and 73.3 %–79.8 % in HPLC, respectively), although not statistically significant (p-values ≥0.1). Mean RCP values remained excellent regardless of heating time (96.9 % vs 97.6 % in TLC and 94.3 vs 95.1 in HPLC, respectively). Therefore, in view of the short half-life of ^{68}Ga, a radiolabeling time of 8 min was maintained for the following assays.

As shown in Fig. 5, mean RCP of the [^{68}Ga]Ga-FAPI-46 final product

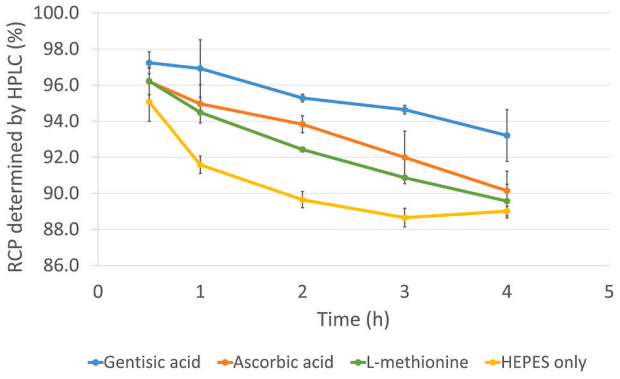

Fig. 5. Time course of [^{68}Ga]Ga-FAPI-46 RCP measured by HPLC, with or without anti-radiolysis compounds.

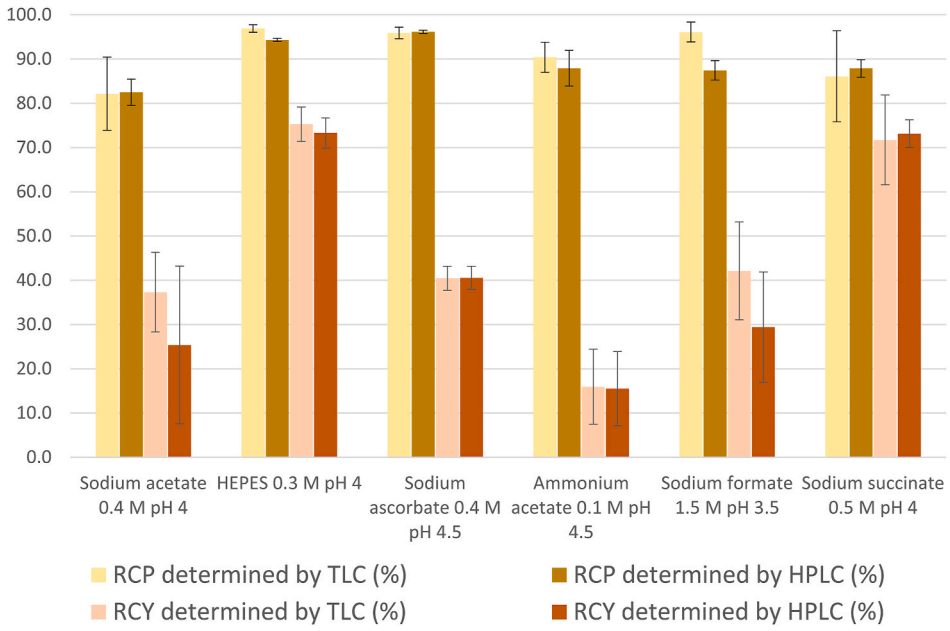

Fig. 4. Mean RCP and RCY values obtained by TLC and HPLC during the study of the influence of the reaction buffer on the radiolabeling of [^{68}Ga]Ga-FAPI-46.

slightly decreased over time (from approximately 95 %–89 % over 4 h). Addition of 0.1 mL ascorbic acid or methionine 10 mg/mL slightly increased the stability of the final product over time, but only for early time points (from 1 h to 3 h), as the mean RCP at 4 h was also around 90 % in these conditions. Of note, the alpha-amino acid motif of methionine did not seem to form undesired complexes with ^{68}Ga, as it can be observed with glycine (Bianco et al., 1975). This is possibly due to the electron-withdrawing effect of the thioether group, making the amine and carboxylic acid protons more acidic, which would decrease the stability of methionine metal complexes (Yamauchi and Odani, 1996). Interestingly, a final concentration of 0.6 mg/mL gentisic acid in the reaction medium and in the final product allowed slightly better RCP over time (mean 97.2 % at 0.5 h with 4 % decrease over 4 h, vs around 6 % decrease over 4 h with ascorbic acid and methionine). Moreover, mean RCY determined by HPLC was excellent in the presence of gentisic acid, reaching the same 79.8 % value than with 16 min heating time. As a strong antioxidant and free-radical scavenger (Joshi et al., 2012), gentisic acid was first used as a radiostabilizer in ^{99m}Tc radiopharmaceuticals (Tofe et al., 1980; Ballinger et al., 1981) and showed particular relevance in the labeling of radiosensitive compounds, such as peptides or proteins (Liu and Edwards, 2001; Trindade and Balter, 2020). Also reported in automated ^{68}Ga radiolabeling protocols (Velikyan et al., 2017, 2020; Haskali, 2019; Wagner et al., 2020), gentisic acid was retained for the preparation of [^{68}Ga]Ga-FAPI-46 as it slightly improves the overall synthesis outcome (e.g. the RCP values obtained by TLC, see Fig. 6).

Lower amounts of FAPI-46 involved in the reaction were then investigated in order to increase specific activity (SA, i.e. the amount of radioactivity per unit mass of FAPI-46) of the final product. As a receptor-binding radiopharmaceutical, [^{68}Ga]Ga-FAPI-46 would benefit from a high SA, which would be associated with optimal biodistribution and homogeneous target binding intensity (Kiessling et al., 2017). For SA calculations, the total mass of peptide involved in the radiolabeling was considered as recovered, and the part of activity effectively vectorized was considered as the total activity in the product vial adjusted by the RCP. Radiolabeling assays with 30 µg FAPI-46 logically yielded modest SA values, around 12 MBq/µg. The use of 20 µg FAPI-46 increased the SA values by 40 % (~17 MBq/µg) while the use of only 10 µg FAPI-46 increased the SA of the final product by approximately 2.5 fold (around 30 MBq/µg). Nevertheless, this decrease in the amount of vector resulted in lower RCP (especially in HPLC) and therefore reduced RCY, as displayed in Fig. 7. One of the possible reasons for decreased RCP associated with smaller amounts of vector has been identified in HPLC, with the formation of a radioactive impurity (Radio-impurity 2 in Fig. 8) in all the more important proportions that the amount of FAPI-46 engaged in the reaction was low. Therefore, more efficient reaction conditions were preferred over increased SA and 30 µg FAPI-46 were used for the subsequent assays. This amount is comparable (Spreckelmeyer et al., 2020a) or lower (Alfteimi et al., 2022; Nader et al., 2022) to those reported in the literature; in addition, reduced amounts of FAPI-46 may be specifically considered in particular cases, e.g. if the radiolabeling protocol needs to be adjusted for preclinical applications (International Atomic Energy Agency, 2023). Moreover, as the experiments were conducted with a 7 months-old ^{68}Ge/^{68}Ga generator (7 months past its 1.85 GBq activity reference time), higher SA values can reasonably be expected with a generator of higher calibration.

Finally, the purification applied to the reaction medium following radiolabeling was studied. Without purification, about 15 % of free $^{68}Ga^{3+}$ and radio-impurities was found in the final product (Table 2, Fig. 9A), encouraging the set-up of a post-synthesis "bind-and-elute" approach involving a SPE cartridge. The use of either a Sep-Pak® C_{18} (containing a silica-based, trifunctionally bonded C_{18} solid phase) or an Oasis® HLB (containing a hydrophilic-lipophilic balanced copolymeric

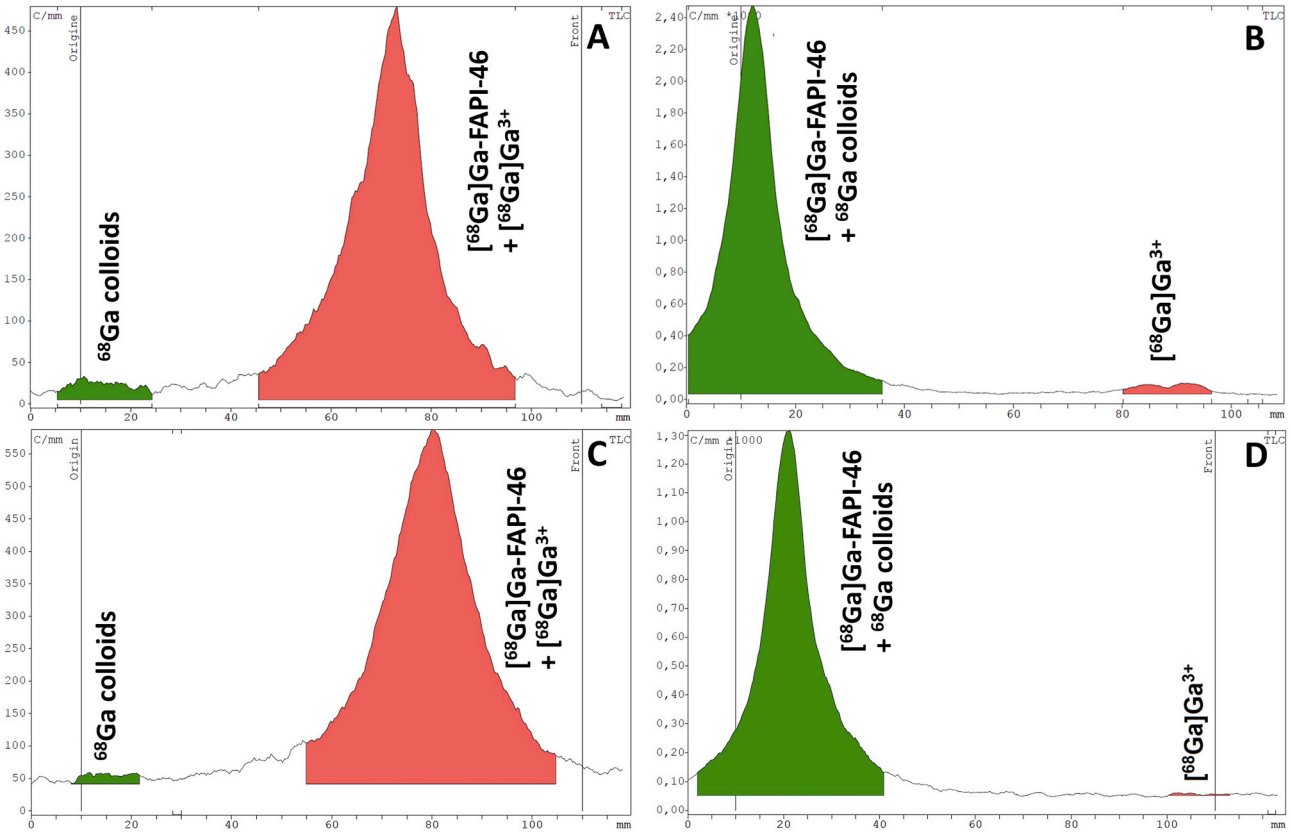

Fig. 6. Radio-TLC spectra of [^{68}Ga]Ga-FAPI-46 after radiolabeling with HEPES 0.3 M (**A**, **B**) or with HEPES 0.3 M + gentisic acid 0.6 mg/mL (**C**, **D**) and elution of the TLC plate with aqueous 0.1 M sodium citrate pH 5 (**B**, **D**) or with aqueous 1 M ammonium acetate in methanol (1:1) (**A**, **C**).

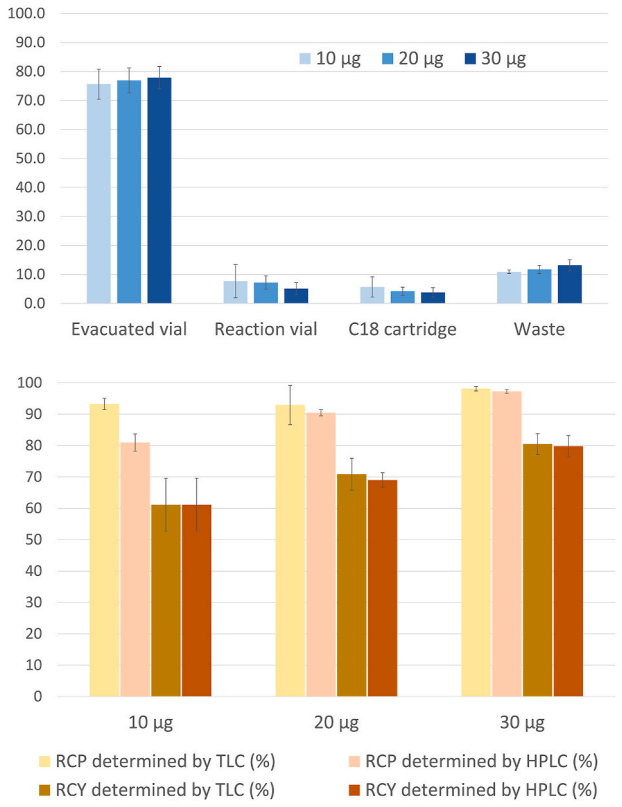

Fig. 7. Activity distribution in the cassette and mean RCP and RCY values obtained by radio-TLC and radio-HPLC depending on the amount of FAPI-46 used for the radiolabeling reaction.

solid phase) cartridge allowed comparable high RCP and RCY, with slightly better results obtained after C_{18} purification (Fig. 9B). Noteworthy, only negligible amounts of radioactivity (around 6 MBq) remained on both cartridges type after elution with 1.5 mL of 60 % ethanol and 8.6 mL of 0.9 % NaCl alternating. A technique associating sequential SPE and QMA cartridge already reported in the literature (Da Pieve et al., 2022) was also investigated, in order to retain the unlabeled FAPI-46 via the free carboxylate arms of the DOTA chelator and thus increase SA. RCP values obtained with this method and with a single Sep-Pak® C_{18} cartridge were comparable (~97 %) but with a slightly cleaner HPLC profile using the Sep-Pak® C_{18} alone (Fig. 9B and C). This dual-cartridges methods that could increase SA would be, as mentioned above, particularly appropriate for preclinical applications. Thus, in view of the excellent results obtained with Sep-Pak® C_{18} alone, this terminal purification method was chosen as the most convenient and effective. This is the most widely reported SPE technique in the literature, especially for automated radiolabeling protocols of small molecules such as [^{68}Ga]Ga-RGD derivatives (Pohle, 2012; Martin, 2014), [^{68}Ga]Ga-PSMA-11 (Reverchon et al., 2020; Kleynhans et al., 2020; Calderoni et al., 2020) or [^{68}Ga]Ga-pentixafor (Sammartano et al., 2020; Spreckelmeyer et al., 2020b; Daniel et al., 2023). Nevertheless, some methods indicate the use of Oasis HLB cartridges, particularly for ^{68}Ga radiolabeling of FAPI-46 (Alfteimi et al., 2022; Da Pieve et al., 2022;

Table 2
Influence of the terminal SPE purification method on the RCP and RCY of [^{68}Ga]Ga-FAPI-46 preparations.

Cartridge(s)	Mean residual activity on the cartridge		TLC measurements		HPLC measurements	
	MBq ± SD	% ± SD	Mean RCP ± SD (%)	Mean RCY ± SD (%)	Mean RCP ± SD (%)	Mean RCY ± SD (%)
None	–	–	85.5 ± 3.9	82.0 ± 4.0	85.1 ± 2.8	81.6 ± 3.0
Sep-Pak® C18	5.7 ± 0.5	1.3 ± 0.1	98.1 ± 0.7	80.6 ± 3.3	97.3 ± 0.6	79.9 ± 3.4
Oasis® HLB	7.0 ± 0.6	1.8 ± 0.2	98.2 ± 0.4	73.3 ± 1.0	98.4 ± 0.3	73.4 ± 1.0
Sep-Pak® C18 + QMA (sequential)	6.0 ± 0.5 13.5 ± 1.0	1.5 ± 0.1 3.3 ± 0.2	96.4 ± 2.8	80.1 ± 1.5	98.3 ± 0.6	81.7 ± 1.3

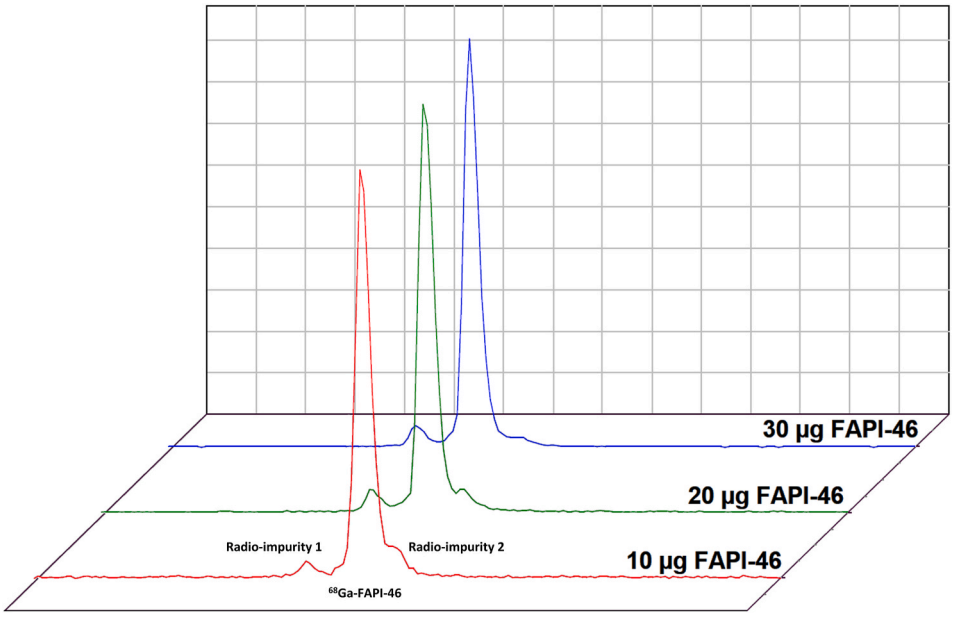

Fig. 8. Radio-HPLC chromatograms showing the RCP of [^{68}Ga]Ga-FAPI-46 after purification, depending on the amount of vector involved in the radiolabeling reaction.

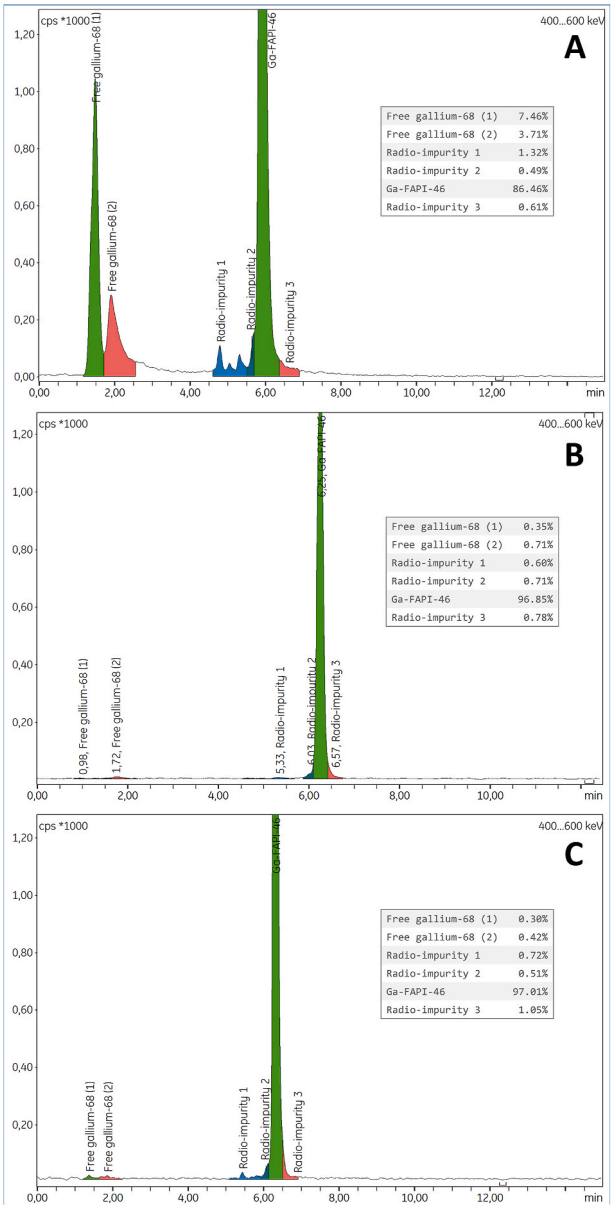

Fig. 9. Radio-HPLC chromatograms showing the RCP of [^{68}Ga]Ga-FAPI-46 without SPE purification (**A**), after Sep-Pak® C_{18} cartridges (**B**) or after sequential Sep-Pak® C_{18} and QMA cartridges (**C**).

Nader et al., 2022).

Overall, the best ^{68}Ga radiolabeling conditions for FAPI-46 were identified as 30 μg of vector, HEPES buffer 0.3 M pH 4, 8 min heating and purification on a Sep-Pak® C_{18} cartridge. Mains quality controls results for three [^{68}Ga]Ga-FAPI-46 test batches using these conditions are presented, in Table 3. One of the limitations of this automated sequence is its suitability only for the GALLI AD® generator and its 1.1 mL eluate. Nevertheless, if another generator should be used (e.g. Galliapharm®), it would be conceivable to add during the first part of the automated synthesis an additional post-elution processing step involving a strong cation exchange (SCX) cartridge that would be eluted with 1.1 mL of NaCl 5 M in HCl 0.1 N (Martin, 2014). This extra step would overcome the initial volume of the ^{68}Ga solution and eliminate metallic impurities in the eluate resulting from the column, the eluent or the nuclear decay of ^{68}Ga that could, if present, interfere with the labeling reaction (Meyer et al., 2004; Velikyan, 2015; Zhernosekov et al., 2007).

Table 3
Mains quality control results for three [^{68}Ga]Ga-FAPI-46 test batches using the optimal reaction conditions (30 μg of vector, HEPES buffer 0.3 M pH 4, 8 min heating and SPE purification on a Sep-Pak® C18 cartridge).

Test	Batch 1	Batch 2	Batch 3
Appearance	Clear, colorless solution	Clear, colorless solution	Clear, colorless solution
pH	6	6	6
Radiochemical purity			
[^{68}Ga]Ga-FAPI-46 (HPLC)	97.9 %	97.2 %	96.7 %
Free gallium-68 (HPLC)	0.1 %	0.3 %	0.3 %
[^{68}Ga]gallium impurities (HPLC)	2.0 %	2.5 %	3.0 %
[^{68}Ga]Ga-FAPI-46 (TLC)	98.4 %	98.6 %	97.3 %
[^{68}Ga]gallium impurities (TLC)	1.6 %	1.4 %	2.7 %
Filter integrity test	Passed	Passed	Passed
Radioactivity	397 MBq	363 MBq	350 MBq
Specific activity	13.2 MBq/μg	12.1 MBq/μg	11.7 MBq/μg
Molar activity	11.7 GBq/μmol	10.7 GBq/μmol	10.4 GBq/μmol
Radiochemical yield (TLC)	83.9 %	80.5 %	77.2 %
(HPLC)	83.4 %	79.3 %	76.7 %
Stability over 4h (HPLC)	≥91.6 %	≥93.6 %	≥94.4 %

4. Conclusion

Molecular imaging of the tumor microenvironment by targeting FAP has shown an undeniable interest in both oncology and non-cancer diseases. This is illustrated by the recent development of innovative vector molecules in this application (Greifenstein et al., 2022), some with potential theranostic purposes (Bartoli et al., 2022). In the present work, an optimized protocol for automated production of [^{68}Ga]Ga-FAPI-46 on a GAIA® synthesis module was developed through an in-depth study of several reaction parameters. The automated process being GMP-compliant, the use of GMP-grade FAPI-46 associated with the development and validation of additional quality controls (sterility, bacterial endotoxins and generator radionuclidic purity) would allow translation to the clinic.

CRediT authorship contribution statement

Léa Rubira: Writing – original draft, Investigation. **Charlotte Donzé:** Writing – review & editing. **Juliette Fouillet:** Investigation. **Benjamin Algudo:** Investigation. **Pierre Olivier Kotzki:** Visualization. **Emmanuel Deshayes:** Writing – review & editing. **Cyril Fersing:** Writing – original draft, Supervision, Methodology, Investigation, Conceptualization.

Declaration of competing interest

The authors declare that they have no known competing financial interests or personal relationships that could have appeared to influence the work reported in this paper.

Data availability

No data was used for the research described in the article.

Acknowledgement

This research did not receive any specific grant from funding agencies in the public, commercial, or not-for-profit sectors. The authors thank Malissone Viarasakd and Fiona Garnier for their help in the completion of this work.

Appendix A. Supplementary data

Supplementary data to this article can be found online at https://doi.org/10.1016/j.apradiso.2024.111211.

References

Alfteimi, A., Lützen, U., Helm, A., Jüptner, M., Marx, M., Zhao, Y., Zuhayra, M., 2022. Automated synthesis of [68Ga]Ga-FAPI-46 without pre-purification of the generator eluate on three common synthesis modules and two generator types. EJNMMI radiopharm. chem. 7, 20. https://doi.org/10.1186/s41181-022-00172-1.

Antunes, I.F., Franssen, G.M., Zijlma, R., Laverman, P., Boersma, H.H., Elsinga, P.H., 2020. New sensitive method for HEPES quantification in 68Ga-radiopharmaceuticals. EJNMMI radiopharm. chem. 5, 12. https://doi.org/10.1186/s41181-020-00093-x.

Ballinger, J., Der, M., Bowen, B., 1981. Stabilization of 99mTc-pyrophosphate injection with gentisic acid. Eur. J. Nucl. Med. 6, 153–154. https://doi.org/10.1007/BF00253164.

Bartoli, F., Elsinga, P., Nazario, L.R., Zana, A., Galbiati, A., Millul, J., Migliorini, F., Cazzamalli, S., Neri, D., Slart, R.H.J.A., Erba, P.A., 2022. Automated radiosynthesis, Preliminary in vitro/in vivo Characterization of OncoFAP-based radiopharmaceuticals for cancer imaging and therapy. Pharmaceuticals 15, 958. https://doi.org/10.3390/ph15080958.

Baum, R.P., Rösch, F. (Eds.), 2013. Theranostics, Gallium-68, and Other Radionuclides: A Pathway to Personalized Diagnosis and Treatment, Recent Results in Cancer Research. Springer Berlin Heidelberg, Berlin, Heidelberg. https://doi.org/10.1007/978-3-642-27994-2.

Baur, B., Solbach, C., Andreolli, E., Winter, G., Machulla, H.-J., Reske, S., 2014. Synthesis, radiolabelling and in vitro characterization of the gallium-68-, yttrium-90- and lutetium-177-labelled PSMA ligand. CHX-A''-DTPA-DUPA-Pep. Pharmaceuticals 7, 517–529. https://doi.org/10.3390/ph7050517.

Bauwens, M., Chekol, R., Vanbilloen, H., Bormans, G., Verbruggen, A., 2010. Optimal buffer choice of the radiosynthesis of 68Ga–Dotatoc for clinical application. Nucl. Med. Commun. 31, 753–758. https://doi.org/10.1097/MNM.0b013e32833acb99.

Bianco, P., Haladjian, J., Pilard, R., 1975. Complexation du gallium par la glycine ou l'isoleucine. Journal of the Less Common Metals 42, 127–135. https://doi.org/10.1016/0022-5088(75)90026-0.

Calderoni, L., Farolfi, A., Pianori, D., Maietti, E., Cabitza, V., Lambertini, A., Ricci, G., Telo, S., Lodi, F., Castellucci, P., Fanti, S., 2020. Evaluation of an automated module synthesis and a sterile Cold kit–based preparation of ^{68} Ga-PSMA-11 in Patients with Prostate cancer. J. Nucl. Med. 61, 716–722. https://doi.org/10.2967/jnumed.119.231605.

Cankaya, A., Balzer, M., Amthauer, H., Brenner, W., Spreckelmeyer, S., 2023. Optimization of 177Lu-labelling of DOTA-TOC, PSMA-I&T and FAPI-46 for clinical application. EJNMMI radiopharm. chem. 8, 10. https://doi.org/10.1186/s41181-023-00196-1.

Da Pieve, C., Costa Braga, M., Turton, D.R., Valla, F.A., Cakmak, P., Plate, K.-H., Kramer-Marek, G., 2022. New fully automated preparation of high apparent molar activity 68Ga-FAPI-46 on a Trasis AiO platform. Molecules 27, 675. https://doi.org/10.3390/molecules27030675.

Daniel, T., Balouzet Ravinet, C., Clerc, J., Batista, R., Mouraeff, Y., 2023. Automated synthesis and quality control of [68Ga]Ga-PentixaFor using the Gaia/Luna Elysia-Raytest module for CXCR4 PET imaging. EJNMMI radiopharm. chem. 8, 4. https://doi.org/10.1186/s41181-023-00187-2.

Davey, P.R.W.J., Paterson, B.M., 2022. Modern developments in Bifunctional chelator design for gallium radiopharmaceuticals. Molecules 28, 203. https://doi.org/10.3390/molecules28010203.

de Blois, E., de Zanger, R.M.S., Oehlke, E., Chan, H.S., Breeman, W.A.P., 2018. Semi-automated system for concentrating 68Ga-eluate to obtain high molar and volume concentration of 68Ga-Radiopharmaca for preclinical applications. Nucl. Med. Biol. 6, 16–21. https://doi.org/10.1016/j.nucmedbio.2018.06.006.

Decristoforo, C., 2012. Gallium-68 - a new opportunity for PET available from a long shelf-life generator - Automation and applications. Curr Radiopharm 5, 212–220. https://doi.org/10.2174/1874471011205030212.

Decristoforo, C., Penuelas, I., Patt, M., Todde, S., 2017. European regulations for the introduction of novel radiopharmaceuticals in the clinical setting. Q. J. Nucl. Med. Mol. Imaging 61, 135–144. https://doi.org/10.23736/S1824-4785.17.02965-X.

Eryilmaz, K., Kilbas, B., 2021. Fully-automated synthesis of 177Lu labelled FAPI derivatives on the module modular lab-Eazy. EJNMMI radiopharm. chem. 6, 16. https://doi.org/10.1186/s41181-021-00130-3.

European Directorate for the Quality of Medicines & Healthcare (Edqm), 2022. Gallium (68Ga) edotreotide injection. European Pharmacopoeia 11 (0 2482), 1274–1276.

European Directorate for the Quality of Medicines & Healthcare (Edqm), 2021. Gallium (68Ga) PSMA-11 injection. European Pharmacopoeia 11 (0), 1276–1277, 3044.

Ferreira, C.M.H., Pinto, I.S.S., Soares, E.V., Soares, H.M.V.M., 2015. (Un)suitability of the use of pH buffers in biological, biochemical and environmental studies and their interaction with metal ions – a review. RSC Adv. 5, 30989–31003. https://doi.org/10.1039/C4RA15453C.

Garcia-Arguello, S.F., Lopez-Lorenzo, B., Ruiz-Cruces, R., 2019. Automated production of [^{68} Ga]Ga-DOTANOC and [^{68} Ga]Ga-PSMA-11 using a TRACERlab FX $_{FN}$ synthesis module. J. Label. Compd. Radiopharm. 62, 146–153. https://doi.org/10.1002/jlcr.3706.

Greifenstein, L., Kramer, C.S., Moon, E.S., Rösch, F., Klega, A., Landvogt, C., Müller, C., Baum, R.P., 2022. From automated synthesis to in vivo application in Multiple types of cancer—clinical results with [68Ga]Ga-DATA5m. SA.FAPi. Pharmaceuticals 15, 1000. https://doi.org/10.3390/ph15081000.

Greiser, J., Winkens, T., Perkas, O., Kuehnel, C., Weigand, W., Freesmeyer, M., 2022. Automated GMP production and preclinical evaluation of [68Ga]Ga-TEoS-DAZA and [68Ga]Ga-TMoS-DAZA. Pharmaceutics 14, 2695. https://doi.org/10.3390/pharmaceutics14122695.

Haskali, M.B., 2019. Automated preparation of clinical grade [68Ga]Ga-DOTA-CP04, a cholecystokinin-2 receptor agonist, using iPHASE MultiSyn synthesis platform. EJNMMI Radiopharmacy and Chemistry 4, 23.

Hendrikse, H., Kiss, O., Kunikowska, J., Wadsak, W., Decristoforo, C., Patt, M., 2022. EANM position on the in-house preparation of radiopharmaceuticals. Eur J Nucl Med Mol Imaging 49, 1095–1098. https://doi.org/10.1007/s00259-022-05694-z.

Hörmann, A.A., Plhak, E., Klingler, M., Rangger, C., Pfister, J., Schwach, G., Kvaternik, H., von Guggenberg, E., 2022. Automated synthesis of 68Ga-labeled DOTA-MGS8 and preclinical Characterization of cholecystokinin-2 receptor targeting. Molecules 27, 2034. https://doi.org/10.3390/molecules27062034.

Huang, R., Pu, Yu, Huang, S., Yang, C., Yang, F., Pu, Yongzhu, Li, J., Chen, L., Huang, Y., 2022. FAPI-PET/CT in cancer imaging: a potential novel molecule of the Century. Front. Oncol. 12.

International Atomic Energy Agency, 2023. Guidance for Preclinical Studies with Radiopharmaceuticals, vol. 8. IAEA Radioisotopes And Radiopharmaceuticals Series No.

Jansen, K., Heirbaut, L., Cheng, J.D., Joossens, J., Ryabtsova, O., Cos, P., Maes, L., Lambeir, A.-M., De Meester, I., Augustyns, K., Van der Veken, P., 2013. Selective inhibitors of fibroblast activation protein (FAP) with a (4-Quinolinoyl)-glycyl-2-cyanopyrrolidine Scaffold. ACS Med. Chem. Lett. 4, 491–496. https://doi.org/10.1021/ml300410d.

Jansen, K., Heirbaut, L., Verkerk, R., Cheng, J.D., Joossens, J., Cos, P., Maes, L., Lambeir, A.-M., De Meester, I., Augustyns, K., Van der Veken, P., 2014. Extended structure–activity relationship and Pharmacokinetic investigation of (4-Quinolinoyl) glycyl-2-cyanopyrrolidine inhibitors of fibroblast activation protein (FAP). J. Med. Chem. 57, 3053–3074. https://doi.org/10.1021/jm500031w.

Joshi, R., Gangabhagirathi, R., Venu, S., Adhikari, S., Mukherjee, T., 2012. Antioxidant activity and free radical scavenging reactions of gentisic acid: *in-vitro* and pulse radiolysis studies. Free Radic. Res. 46, 11–20. https://doi.org/10.3109/10715762.2011.633518.

Kiessling, F., Pichler, B.J., Hauff, P. (Eds.), 2017. Small Animal Imaging. Springer International Publishing, Cham. https://doi.org/10.1007/978-3-319-42202-2.

Kleynhans, J., Rubow, S., le Roux, J., Marjanovic-Painter, B., Zeevaart, J.R., Ebenhan, T., 2020. Production of [^{68} Ga]Ga-PSMA: Comparing a manual kit-based method with a module-based automated synthesis approach. J. Label. Compd. Radiopharm. https://doi.org/10.1002/jlcr.3879.

Lepareur, N., 2022. Cold kit labeling: the Future of 68Ga radiopharmaceuticals? Front. Med. 9, 812050 https://doi.org/10.3389/fmed.2022.812050.

Liang, L., Li, W., Li, X., Jin, X., Liao, Q., Li, Y., Zhou, Y., 2022. 'Reverse Warburg effect' of cancer-associated fibroblasts. Int. J. Oncol. 60, 67. https://doi.org/10.3892/ijo.2022.5357 (Review).

Lindner, T., Loktev, A., Giesel, F., Kratochwil, C., Altmann, A., Haberkorn, U., 2019. Targeting of activated fibroblasts for imaging and therapy. EJNMMI radiopharm. chem. 4, 16. https://doi.org/10.1186/s41181-019-0069-0.

Liu, S., Edwards, D.S., 2001. Stabilization of ^{90} Y-labeled DOTA-Biomolecule Conjugates using gentisic acid and ascorbic acid. Bioconjugate Chem. 12, 554–558. https://doi.org/10.1021/bc000145v.

Loktev, A., Lindner, T., Burger, E.-M., Altmann, A., Giesel, F., Kratochwil, C., Debus, J., Marmé, F., Jäger, D., Mier, W., Haberkorn, U., 2019. Development of fibroblast activation protein–targeted Radiotracers with improved tumor Retention. J. Nucl. Med. 60, 1421–1429. https://doi.org/10.2967/jnumed.118.224469.

Martin, R., 2014. Cationic eluate pretreatment for automated synthesis of [68Ga] CPCR4.2. Nucl. Med. Biol. 6.

Meisenheimer, M., Kürpig, S., Essler, M., Eppard, E., 2020. Manual vs automated ^{68} Ga-radiolabelling-A comparison of optimized processes. J Label Compd Radiopharm 63, 162–173. https://doi.org/10.1002/jlcr.3821.

Meyer, G.-J., Mäcke, H., Schuhmacher, J., Knapp, W.H., Hofmann, M., 2004. 68Ga-labelled DOTA-derivatised peptide ligands. Eur J Nucl Med Mol Imaging 31, 1097–1104. https://doi.org/10.1007/s00259-004-1486-0.

Migliari, S., Scarlattei, M., Baldari, G., Ruffini, L., 2023. Scale down and optimized automated production of [68Ga]68Ga-DOTA-ECL1i PET tracer targeting CCR2 expression. EJNMMI radiopharm. chem. 8, 3. https://doi.org/10.1186/s41181-023-00188-1.

Migliari, S., Scarlattei, M., Baldari, G., Silva, C., Ruffini, L., 2022. A specific HPLC method to determine residual HEPES in [68Ga]Ga-radiopharmaceuticals: development and validation. Molecules 27, 4477. https://doi.org/10.3390/molecules27144477.

Nader, M., Valla, D.F., Vriamont, C., Masset, J., Pacelli, A., Herrmann, K., Zarrad, F., 2022. [68Ga]/[90Y]FAPI-46: automated production and analytical validation of a theranostic pair. Nucl. Med. Biol. 110–111, 37–44. https://doi.org/10.1016/j.nucmedbio.2022.04.010.

Nelson, B.J.B., Andersson, J.D., Wuest, F., Spreckelmeyer, S., 2022. Good practices for 68Ga radiopharmaceutical production. EJNMMI radiopharm. chem. 7, 27. https://doi.org/10.1186/s41181-022-00180-1.

Pisaneschi, F., Viola, N.T., 2022. Development and validation of a PET/SPECT radiopharmaceutical in oncology. Mol Imaging Biol 24, 1–7. https://doi.org/10.1007/s11307-021-01645-6.

Plhak, E., Pichler, C., Dittmann-Schnabel, B., Gößnitzer, E., Aigner, R.M., Stanzel, S., Kvaternik, H., 2023. Automated synthesis of [68Ga]Ga-FAPI-46 on a Scintomics GRP synthesizer. Pharmaceuticals 16, 1138. https://doi.org/10.3390/ph16081138.

Pohle, K., 2012. 68Ga-NODAGA-RGD is a suitable substitute for 18F-Galacto-RGD and can be produced with high specific activity in a cGMP/GRP compliant automated process. Nucl. Med. Biol. 8.

Privé, B.M., Boussihmad, M.A., Timmermans, B., van Gemert, W.A., Peters, S.M.B., Derks, Y.H.W., van Lith, S.A.M., Mehra, N., Nagarajah, J., Heskamp, S., Westdorp, H., 2023. Fibroblast activation protein-targeted radionuclide therapy: background, opportunities, and challenges of first (pre)clinical studies. Eur J Nucl Med Mol Imaging. https://doi.org/10.1007/s00259-023-06144-0.

Promteangtrong, C., Siripongsatian, D., Jantarato, A., Kunawudhi, A., Kiatkittikul, P., Yaset, S., Boonkawin, N., Chotipanich, C., 2022. Head-to-Head Comparison of 68Ga-FAPI-46 and 18F-FDG PET/CT for evaluation of Head and Neck Squamous cell Carcinoma: a single-Center Exploratory study. J. Nucl. Med. 63, 1155–1161. https://doi.org/10.2967/jnumed.121.262831.

Reverchon, J., Khayi, F., Roger, M., Moreau, A., Kryza, D., 2020. Optimization of the radiosynthesis of [68Ga]Ga-PSMA-11 using a Trasis MiniAiO synthesizer: do we need to heat and purify? Nucl. Med. Commun. 41, 977–985. https://doi.org/10.1097/MNM.0000000000001233.

Sammartano, A., Migliari, S., Scarlattei, M., Baldari, G., Ruffini, L., 2020. Synthesis, validation and quality controls of [68Ga]-DOTA- Pentixafor for PET imaging of chemokine receptor CXCR4 expression. Acta Biomed., e2020097 https://doi.org/10.23750/abm.v91i4.9106.

Scanlan, M.J., Raj, B.K., Calvo, B., Garin-Chesa, P., Sanz-Moncasi, M.P., Healey, J.H., Old, L.J., Rettig, W.J., 1994. Molecular cloning of fibroblast activation protein alpha, a member of the serine protease family selectively expressed in stromal fibroblasts of epithelial cancers. Proc. Natl. Acad. Sci. U.S.A. 91, 5657–5661. https://doi.org/10.1073/pnas.91.12.5657.

Siripongsatian, D., Promteangtrong, C., Kunawudhi, A., Kiatkittikul, P., Boonkawin, N., Chinnanthachai, C., Jantarato, A., Chotipanich, C., 2022. Comparisons of Quantitative parameters of Ga-68-Labelled fibroblast activating protein inhibitor (FAPI) PET/CT and [18F]F-FDG PET/CT in Patients with liver malignancies. Mol Imaging Biol 24, 818–829. https://doi.org/10.1007/s11307-022-01732-2.

Spreckelmeyer, S., Balzer, M., Poetzsch, S., Brenner, W., 2020a. Fully-automated production of [68Ga]Ga-FAPI-46 for clinical application. EJNMMI radiopharm. chem. 5, 31. https://doi.org/10.1186/s41181-020-00112-x.

Spreckelmeyer, S., Schulze, O., Brenner, W., 2020b. Fully-automated production of [68Ga]Ga-PentixaFor on the module modular lab-PharmTracer. EJNMMI radiopharm. chem. 5, 8. https://doi.org/10.1186/s41181-020-0091-2.

Tofe, A.J., Bevan, J.A., Fawzi, M.B., Francis, M.D., Silberstein, E.B., Alexander, G.A., Gunderson, D.E., Blair, K., 1980. Gentisic acid: a new stabilizer for low tin skeletal imaging agents: concise communication. J. Nucl. Med. 21, 366–370.

Trindade, V., Balter, H., 2020. Oxidant and antioxidant effects of gentisic acid in a ^{177} Lu-labelled methionine-containing Minigastrin Analogue. CRP 13, 107–119. https://doi.org/10.2174/1874471012666190916112904.

Velikyan, I., 2015. 68Ga-Based radiopharmaceuticals: production and application relationship. Molecules 20, 12913–12943. https://doi.org/10.3390/molecules200712913.

Velikyan, I., Doverfjord, J.G., Estrada, S., Steen, H., Van Scharrenburg, G., Antoni, G., 2020. GMP production of [68Ga]Ga-BOT5035 for imaging of liver fibrosis in microdosing phase 0 study. Nucl. Med. Biol. 88 (89), 73–85.

Velikyan, I., Rosenstrom, U., Eriksson, O., 2017. Fully automated GMP production of [68Ga]Ga-DO3A-VS-Cys40-Exendin-4 for clinical use. Am J Nucl Med Mol Imaging 7, 111–125.

Wagner, M., Doverfjord, J.G., Tillner, J., Antoni, G., Haack, T., Bossart, M., Laitinen, I., Johansson, L., Pierrou, S., Eriksson, O., Velikyan, I., 2020. Automated GMP-compliant production of [68Ga]Ga-DO3A-Tuna-2 for PET microdosing studies of the Glucagon receptor in humans. Pharmaceuticals 13, 176. https://doi.org/10.3390/ph13080176.

Wegen, S., Roth, K.S., Weindler, J., Claus, K., Linde, P., Trommer, M., Akuamoa-Boateng, D., van Heek, L., Baues, C., Schömig-Markiefka, B., Schomäcker, K., Fischer, T., Drzezga, A., Kobe, C., Köhler, C., Marnitz, S., 2023. First clinical experience with [68Ga]Ga-FAPI-46-PET/CT versus [18F]F-FDG PET/CT for Nodal Staging in Cervical cancer. Clin. Nucl. Med. 48, 150–155. https://doi.org/10.1097/RLU.0000000000004505.

Wegen, S., van Heek, L., Linde, P., Claus, K., Akuamoa-Boateng, D., Baues, C., Sharma, S. J., Schomäcker, K., Fischer, T., Roth, K.S., Klußmann, J.P., Marnitz, S., Drzezga, A., Kobe, C., 2022. Head-to-Head Comparison of [68Ga]Ga-FAPI-46-PET/CT and [18F]F-FDG-PET/CT for Radiotherapy Planning in Head and Neck cancer. Mol Imaging Biol 24, 986–994. https://doi.org/10.1007/s11307-022-01749-7.

Yamauchi, O., Odani, A., 1996. Stability constants of metal complexes of amino acids with charged side chains - Part I: Positively charged side chains (Technical Report). Pure Appl. Chem. 68, 469–496. https://doi.org/10.1351/pac199668020469.

Zhang, J., Singh, A., Kulkarni, H.R., Schuchardt, C., Müller, D., Wester, H.-J., Maina, T., Rösch, F., van der Meulen, N.P., Müller, C., Mäcke, H., Baum, R.P., 2019. From Bench to Bedside—the Bad Berka experience with first-in-human studies. Semin. Nucl. Med. 49, 422–437. https://doi.org/10.1053/j.semnuclmed.2019.06.002.

Zhernosekov, K.P., Filosofov, D.V., Baum, R.P., Aschoff, P., Bihl, H., Razbash, A.A., Jahn, M., Jennewein, M., Rösch, F., 2007. Processing of generator-produced 68Ga for medical application. J. Nucl. Med. 48, 1741–1748. https://doi.org/10.2967/jnumed.107.040378.